Applied Mathematics & Information Sciences
An International Journal

http://dx.doi.org/10.18576/amis/190301

A Three-Dimensional CQBEM Model for Thermal Stress Sensitivities in Anisotropic Materials

Mohamed A. Fahmy[1,2,*]

[1]Department of Mathematics, Adham University College, Umm Al-Qura University, Adham, Makkah 28653, Saudi Arabia
[2]Faculty of Computers and Informatics, Suez Canal University, New Campus, Ismailia 41522, Egypt

Received: 1 Aug. 2024, Revised: 1 Sep. 2024, Accepted: 1 Oct. 2024.
Published online: 1 May 2025.

Abstract: The fundamental purpose of this article is to propose a three-dimensional (3D) convolution quadrature boundary element method (CQBEM) model for precisely calculating thermal stress sensitivity in anisotropic materials. The volume integral is approximated in a discretized version of the problem, and the singularity along the boundary is handled using the convolution quadrature model. The three-dimensional and time-dependent heat equation is solved using a continuous convolution quadrature, while the temporal convolution integrals are discretized in space using the trapezoidal rule. Iterating through the CQBEM solutions for each point of the convolution quadrature rule provides for efficient convergence to the steady state solution. The model can be used to calculate thermal stress gradients in relation to the geometrical parameter in the parametric design of heterogeneous anisotropic materials.

Keywords: Convolution quadrature method, Boundary element method; Thermal stress sensitivities; Anisotropic materials.

Nomenclature

$*$	Time convolution
∇	Spatial gradient
$\nabla\cdot$	Spatial divergence
$\bar{\alpha}$	Thermal expansion coefficient
β_{ij}	Stress-temperature coefficients
ρ	Density
Φ_e^0	$\in S_h^0(\mathrm{C})$ piecewise constant trial function
Ψ_e^1	$\in S_h^1(\mathrm{C})$ Linear continuous trial functions
C	$\mathrm{C}_d \cup \mathrm{C}_n \cup \mathrm{C}_r$ Boundary
C_d	Dirichlet boundary
C_n	Neumann boundary
C_r	Robin boundary
C_{pjkl}	Constant elastic moduli
c_p	Specific heat constant
$E(e)$	Complete elliptic integral of first kind
$\mathbf{I}$	Identity matrix
$J_i(\sigma_p)$	Jacobi elliptic functions
κ	Thermal conductivity coefficients
m	Runge-Kutta stages
N_Q	Number of integration points
$\mathbf{n}$	Outward normal
p	Runge-Kutta order
$\mathbb{Q}$	Flux fundamental solution
q	Runge-Kutta stage order
$\mathbb{q}(\mathbf{x},\tau)$	Conductive heat fluxes
R	Domain
T	Temperature
T	Temperature fundamental solution
$\bar{\mathbf{T}}$	Traction fundamental solution
T_u	Coupling term
$T_\infty(\mathbf{x})$	Ambient temperature
$\mathfrak{t}(\mathbf{x},\tau)$	Traction vector
$\mathbf{U}$	Displacement fundamental solution
$\mathbf{u}$	Displacement

1. Introduction

The standard method for solving boundary value problems in structural mechanics is to employ partial differential equations using elastic, thermal, electrical, magnetic, and other material properties as parameters, beginning with variational principles. Many elasticity problems can be simplified by expressing the displacement fields as polynomial precise solutions with constant coefficients. In engineering practice, interest in thermal stresses can stem from a variety of factors [1-3]. In the first case, it may be desirable to evaluate the distribution of temperatures within a solid body under specified surface loads. These temperatures are then utilized to determine the stress and general deformation distributions for the stated surface forces and moments. Thermal stress calculations are required in many engineering sectors, including the building, vehicle, and aircraft industries, nuclear reactor design, the microelectronics industry, and a variety of other manufacturing fields [4-6]. Thermal stresses occur in a variety of actual design challenges and can be easily used to build theories related to stability, nonlinear behaviour, fracture, contact phenomena, and so on. Depending on the type of solution required, the initial stress state supplied can be related with medium qualities that may or may not exist [7, 8]. In thermal stress analysis, thermal conductivity

*Corresponding author e-mail: maselim@uqu.edu.sa

causes temperature dispersion, which then defines a heat stress field by solving a purely elastic problem. Three-dimensional thermal stress analysis can be used to forecast the behaviour of materials and structures in a variety of engineering and scientific fields under specific thermal conditions [9, 10].

Anisotropic materials are extensively used in the aircraft industry because of their high strength-to-weight ratio. However, the thermal stresses that result from applying thermal loads to such materials are poorly understood. The current study investigated the influence of several parameters on thermal stress generation in anisotropic materials. General formula for calculating thermal stress sensitivity in parameterized anisotropic materials have been devised. Extensive experimental data was used to assist the determination of required sensitivity values. It was discovered that anisotropic materials had a high strength-to-weight ratio under thermal loads, as well as excellent phasing capabilities. The results also demonstrated that the thermal stress deviator effects depend largely on the individual attributes and, to a lesser extent, on the relevant material properties [11-13].

Anisotropic effects can have a significant impact on temperature response and stress distribution in particular materials, calling into question the utility of using isotropic material models to approximate many real-world engineering problems. However, there are few papers available that describe the sensitivity analysis of thermal stresses in anisotropic materials and provide accurate results. The few extant publications each use their own assumptions and approximations, resulting in limited numerical results. The current boundary sensitivity technique for approximating engineering problems, particularly dynamically large-scale engineering issues, is impracticable for assisting in the identification of anisotropic material properties. Therefore, thermal stress sensitivity to boundary parameters in anisotropic materials are being developed [14,15].

When problems are represented in terms of partial differential equations, boundary element techniques (BEMs) can be used instead of finite element and finite difference methods [16, 17]. This is the case when problems are ill-posed, meaning it is unclear which class of functions a solution is properly defined for, or when singularities must be considered. BEMs are extensively used because they allow you to handle the problem on a curve rather than a full domain [18-20]. The researchers propose a numerical method based on the concept of convolution quadrature in the spatial variables and quadrature rules in the time variable, which permits the BEM to be combined with the proposed described general three-dimensional thermo-elastic model for the evaluation of thermal stresses [21-23]. Lubich's initial proposal for convolution quadrature method (CQM) [24, 25] is limited to a fixed time step size. Lopez-Fernandez and Sauter [26] have extended the generalization to a variable step size; the algorithmic realization can be found in [27]. In [28], it is proposed to extend the Runge-Kutta method for underlying time stepping.

In this paper, we present a numerical approach for computing thermal stress sensitivity that combines convolution quadrature (CQ) with the volume-surface variational formulation of the BEM. The volume integral is approximated in a discretized version of the problem, and the singularity near the boundary is addressed using the convolution quadrature method. These sensitivity analysis concerns are tackled using the three-dimensional convolution quadrature boundary element method (CQBEM), which supports non-uniform time increments. The numerical results demonstrate that the recommended technique works. The convergence behavior is determined, as expected, by either the time stepping method or spatial discretization, based on whether rate is lower. Furthermore, it is demonstrated that the proposed CQBEM technique is preferable in certain situations.

2. Formulation of the problem

The governing equations can be written as follows [29]

$$C_{ijkl}\nabla^2\mathbf{u}(\mathbf{x},\tau) + C_{ijkl}\nabla\nabla\cdot\mathbf{u}(\mathbf{x},\tau) - \beta_{ij}\alpha\nabla T(\mathbf{x},\tau) = 0 \quad (1)$$

$$\kappa\nabla^2 T(\mathbf{x},\tau) - \rho c_p \dot{T}(\mathbf{x},\tau) = 0 \quad (2)$$

The Dirichlet, Neumann, and Robin boundary conditions are given by

$$\boldsymbol{u}(\mathbf{x},\tau) = \mathrm{b}_d(\mathbf{x},\tau)\forall\,\mathbf{x}\in \mathrm{C}_d\times(0,t) \quad (3)$$

$$T(\mathbf{x},\tau) = \bar{\mathrm{b}}_d(\mathbf{x},\tau)\forall\,\mathbf{x}\in \mathrm{C}_d\times(0,t) \quad (4)$$

$$\mathfrak{t}(\mathbf{x},\tau) = T^S u(\mathbf{x},\tau) - \beta_{ij}\,\alpha T(\mathbf{x},\tau)\mathbf{n} \;\; = \mathrm{b}_n(\mathbf{x},\tau)\forall\,\mathbf{x}\in \mathrm{C}_n\times(0,t) \quad (5)$$

$$\mathfrak{q}(\mathbf{x},\tau) = \bar{\mathrm{b}}_n(\mathbf{x},\tau)\forall\,\mathbf{x}\in \mathrm{C}_n\times(0,t) \quad (6)$$

$$\mathfrak{q}(\mathbf{x},\tau) + \kappa(\mathbf{x})T(\mathbf{x},\tau) \; = \bar{\mathrm{b}}_r(\mathbf{x})\forall\,\mathbf{x}\in \mathrm{C}_r\times(0,t) \quad (7)$$

Where

$$\mathfrak{q}(\mathbf{x},\tau) = -\kappa(\mathbf{x})\big(T(\mathbf{x},\tau) - T_\infty(\mathbf{x})\big) \quad (8)$$

And

$$\bar{\mathrm{b}}_r(\mathbf{x}) = \kappa(\mathbf{x})T_\infty(\mathbf{x}) \quad (9)$$

3. Numerical BEM implementation

According to [6, 7], Eq. (1) with the weighted residual formula can be written as follows

$$\int_0^t\int_\Omega \mathbf{G}^{\mathrm{T}}(\mathbf{x}-\mathbf{y},\tau-\bar{\tau})(\mathcal{B}\mathbf{u}^{\mathrm{g}})(\mathbf{y},\tau)\mathrm{d}\Omega = \int_\Omega \mathbf{G}^{\mathrm{T}}(\mathbf{x}-\mathbf{y},\tau) * (\mathcal{B}\mathbf{u}^{\mathrm{g}})(\mathbf{y},\tau)\mathrm{d}\Omega = 0. \quad (10)$$

where $\mathcal{B}$, $\mathcal{B}^*$, and $\mathbf{u}^{\mathrm{g}} = [\mathbf{u}^T T]^T$ are defined there.

Based on the fundamental solutions of [30], the representation formula ($\forall\mathbf{x}\in$ R)

$$\mathbf{u}(x,\tau) = -\int_0^\tau \int_R (\mathcal{B}^*\mathbf{G})^{\mathrm{T}}(\mathbf{x}-\bar{\mathbf{x}},\tau-\bar{\tau})\mathbf{u}^{\mathrm{g}}(\bar{\mathbf{x}},\bar{\tau})\mathrm{dRd}\tau$$

$$+\int_{\mathrm{C}} \left(\mathbf{U}(\mathbf{x}-\bar{\mathbf{x}})\mathbb{t}(\bar{\mathbf{x}},\tau) - \mathrm{T}_u(\mathbf{x}-\bar{\mathbf{x}},\tau) * \mathbb{q}(\bar{\mathbf{x}},\tau)\right)d\mathrm{C}$$

$$-\int_{\mathrm{C}} \left(\bar{\mathbf{T}}(\mathbf{x}-\bar{\mathbf{x}})\mathbf{u}(\bar{\mathbf{x}},\tau) + \mathbb{Q}_u(\mathbf{x}-\bar{\mathbf{x}},\tau) * T(\bar{\mathbf{x}},\tau)\right)d\mathrm{C}. \quad (11)$$

$$T(x,\tau) = -\int_0^\tau \int_R (\mathcal{B}^*\mathbf{G})^{\mathrm{T}}(\mathbf{x}-\bar{\mathbf{x}},\tau-\bar{\tau})\mathbf{u}^{\mathrm{g}}(\bar{\mathbf{x}},\bar{\tau})\mathrm{dRd}\tau$$

$$-\int_{\mathrm{C}} \left(\left(\mathrm{T}(\mathbf{x}-\bar{\mathbf{x}},\tau) * \mathbb{q}(\bar{\mathbf{x}},\tau)\right) + \left(\bar{\mathbb{Q}}(\mathbf{x}-\bar{\mathbf{x}},\tau) * T(\bar{\mathbf{x}},\tau)\right)\right) d\mathrm{C}. \quad (12)$$

Based on the spatial discretization [30], we have $\mathrm{C} = U_i^{N_i}\tau_i$

Hence, we get

$$\mathbf{u}_h(\mathbf{x},\tau) = \sum_{e=1}^{\mathbb{N}_d} \Psi_e^1(\mathbf{x})\mathbf{u}^e(\tau), \quad (13)$$

$$\mathbb{t}_h(\mathbf{x},\tau) = \sum_{e=1}^{\mathbb{N}_n} \Phi_e^0(\mathbf{x})\mathbb{t}^e(\tau) \quad (14)$$

$$T_h(\mathbf{x},\tau) = \sum_{e=1}^{\mathbb{N}_d} \Psi_e^1(\mathbf{x})T^e(\tau) \quad (15)$$

$$\mathbb{q}_h(\mathbf{x},\tau) = \sum_{e=1}^{\mathbb{N}_n} \Phi_e^0(\mathbf{x})\mathbb{q}^e(\tau) \quad (16)$$

The spatially discretized operators are

$$\mathbb{V}_{[nm]} = \int_{\mathrm{supp}\,(\Phi_m^0)} \mathbf{U}(\mathbf{x}_n-\bar{\mathbf{x}})\,\Phi_m^0(\bar{\mathbf{x}})\mathrm{d}\Gamma_{\bar{\mathbf{x}}}, \quad (17)$$

$$\mathbb{V}_{[nm]}^{\theta} = \int_{\mathrm{supp}\,(\Phi_m^0)} \mathrm{T}(\mathbf{x}_n-\bar{\mathbf{x}},\tau)\,\Phi_m^0(\bar{\mathbf{x}})\mathrm{d}\Gamma_{\bar{\mathbf{x}}}, \quad (18)$$

$$\mathbb{V}_{[nm]}^{C} = \int_{\mathrm{supp}\,(\Phi_m^0)} \mathrm{T}_u(\mathbf{x}_n-\bar{\mathbf{x}},\tau)\,\Phi_m^0(\bar{\mathbf{x}})\mathrm{d}\Gamma_{\bar{\mathbf{x}}}, \quad (19)$$

$$\mathbb{K}_{[nm]} = \int_{\mathrm{supp}\,(\Psi_m^1)} \bar{\mathrm{T}}(\mathbf{x}_n-\bar{\mathbf{x}})\Psi_m^1(\bar{\mathbf{x}})\mathrm{d}\Gamma_{\bar{\mathbf{x}}}, \quad (20)$$

$$\mathbb{K}_{[nm]}^{\theta} = \int_{\mathrm{supp}\,(\Psi_m^1)} \mathbb{Q}(\mathbf{x}_n-\bar{\mathbf{x}},\tau)\Psi_m^1(\bar{\mathbf{x}})\mathrm{d}\Gamma_{\bar{\mathbf{x}}}, \quad (21)$$

$$\mathbb{K}_{[nm]}^{C} = \int_{\mathrm{supp}(\Psi_m^1)} \mathbb{Q}_u(\mathbf{x}_n-\bar{\mathbf{x}},\tau)\Psi_m^1(\bar{\mathbf{x}})\mathrm{d}\Gamma_{\bar{\mathbf{x}}} \quad (22)$$

where

$$\mathbb{C}\mathrm{u}(\tau) = \mathbb{V}\,\mathbb{t}(\tau) - \mathbb{K}\,\mathrm{u}(\tau) + \mathbb{V}^{\mathrm{C}}(\tau) * \mathbb{q}(\tau) - \mathbb{K}^{\mathrm{C}}(\tau) * T(\tau) \quad (23)$$

$$\mathbb{C}^T T(\tau) = \mathbb{V}^T(\tau) * \mathbb{q}(\tau) - \mathbb{K}^T(\tau) * T(\tau) \quad (24)$$

Based on [30] and [36], we have

$$y(\tau) = f(\tau) * g(\tau) = \int_0^\tau f(\tau-\bar{\tau})g(\bar{\tau})\mathrm{d}\bar{\tau} = \frac{1}{2\pi\mathrm{i}}\int_C \hat{f}(\mathbb{s})\int_0^t \mathrm{e}^{\mathbb{s}(\tau-\bar{\tau})}g(\bar{\tau})\mathrm{d}\bar{\tau}\mathrm{d}\mathbb{s}\,, \quad (25)$$

where for the Laplace variable holds $\mathbb{s} \in \mathbb{C}$, s.t. $\Re\mathbb{s} > 0$. Equation (25) is only valid if the Laplace transform $\hat{f}(\mathbb{s})$ and its inverse exist.

According to [7], we can write

$$\frac{\partial}{\partial\tau}x(\tau,\mathbb{s}) = sx(\tau,\mathbb{s}) + \mathrm{g}(\tau) \text{ with } x(\tau=0,\mathbb{s}) = 0\,. \quad (26)$$

Assume that we have $(\tau_n)_{n=0}^N$ time steps

$$0 = \tau_0 < \tau_1 < \cdots < \tau_N = t,\ \Delta\tau_n = \tau_n - \tau_{n-1} \quad (27)$$

To solve (18), we use the implicit Euler method with the following approximation

$$x_n = \frac{x_{n-1}}{1-\mathbb{s}\Delta\tau_n} + \frac{\Delta\tau_n}{1-\mathbb{s}\Delta\tau_n}\mathrm{g}_n\,, \quad (28)$$

By using the following discrete values $x_n = x(\tau_n)$ in (17), we obtain

$$y(\tau_n) = f\left(\frac{1}{\Delta\tau_n}\right)\mathrm{g}_n + \frac{1}{2\pi\mathrm{i}}\int_C f(\mathbb{s})\frac{x_{n-1}}{1-\mathbb{s}\Delta\tau_n}\,\mathrm{d}\mathbb{s}. \quad (29)$$

Thus, the ultimate quadrature rule for the convolution integral is

$$y(\tau_n) = \hat{f}\left(\frac{1}{\Delta\tau_n}\right)\mathrm{g}_n + \sum_{p=1}^{N_Q} \mathbb{w}_p \frac{\hat{f}(\mathbb{s}_p)}{1-\mathbb{s}_p\Delta\tau_n}x_{n-1}(\mathbb{s}_p)\,. \quad (30)$$

According to Runge-Kutta methods [27, 28], we obtain

$$\mathbb{s}_p = \lambda(\sigma_p), \mathbb{N}_Q = \mathbb{N}\log^2(\mathbb{N}), \mathbb{w}_p = \frac{4E(e^2)}{1\pi i}\lambda'(\sigma_p),\ E(e) = \int_0^1 \frac{dx}{\sqrt{(1-x^2)(1-e^2x^2)}}, E'(e) = E(1-e),$$

$$e = \frac{\bar{q}-\sqrt{2\bar{q}-1}}{\bar{q}+\sqrt{2\bar{q}-1}},\qquad \bar{q} = \frac{\Delta\tau_{\max}5\max_i|\gamma_i(\mathrm{A})|}{\Delta\tau_{\min}\min_i|\gamma_i(\mathrm{A})|},$$

$$\lambda(\sigma_p) = \frac{1}{\Delta\tau_{min}(\bar{q}-1)}\left(\sqrt{2\bar{q}-1}\frac{e^{-1}+J_1(\sigma_p)}{e^{-1}-J_1(\sigma_p)} - 1\right),$$

$$\lambda'(\sigma_p) = \frac{\sqrt{2\bar{q}-1}}{\Delta\tau_{min}(\bar{q}-1)}\frac{2J_2(\sigma_p)J_3(\sigma_p)}{k\left(e^{-1}-J_1(\sigma_p)\right)^2}$$

and $\sigma_p = -E(e^2) + \left(p-\frac{1}{2}\right)\frac{4E(e^2)}{N_Q} + \frac{i}{2}E'(e^2)\,.$

According to [37], Runge-Kutta method with its Butcher tableau $\frac{c|A}{b^T}$, $\mathcal{R}(\infty) = 0$, and invertible matrix $\mathbb{A} \in \mathbb{R}^{m\times m}$, $\mathrm{b},\mathrm{c} \in \mathbb{R}^m$, is $\mathbb{A}$-stable with $p \geqslant 1$ and $q \leqslant p$ if the stability function $\mathcal{R}(z) = 1 + z\mathbf{t}(I - z\,\mathbb{A})^{-1}\mathbb{1}$, $\mathbb{1} := (1,1,\dots,1)^{\mathrm{T}}$ of size m satisfies $|\mathcal{R}(z)| \leqslant 1$, for $\Re z \leqslant 0$, $|\mathcal{R}(\mathrm{i}y)| < 1$ for $y \neq 0$, and $I - z\mathbb{A}$ is non-singular for $\Re z \leqslant 0$.

Using the vector $\mathbb{g}_n$ the algorithm at the time step n is

- For $n = 1$

$$y(\tau_1) = \hat{f}((\Delta\tau_1\,\mathbb{A})^{-1})\mathbb{g}_1 \quad (31)$$

- For $n = 2,\dots,N$, The algorithm consists of the following two steps:

1. Modify the vector of solution x_{n-1} at every integration point $\mathbb{s}_p$ for $p = 1,\dots,N_Q$

$$x_{n-1}(\mathbb{s}_p) = \left(1-\Delta\tau_{n-1}\mathbb{s}_p\mathbb{A}\right)^{-1}\left(\left(\mathbb{b}^T\mathbb{A}^{-1}\cdot x_{n-2}(\mathbb{s}_p)\right)\mathbb{1} + \Delta\tau_{n-1}\mathbb{A}\mathbb{g}_{n-1}\right) \quad (32)$$

2. Solve the integral at τ_n

$$\mathrm{y}(\tau_n) = \hat{f}((\Delta\tau_n\,\mathrm{A})^{-1})\mathbb{g}_n + \sum_{p=1}^{N_Q} \mathbb{w}_p\,\hat{f}(\mathbb{s}_p)\left(\mathbb{b}^{\mathrm{T}}\mathbb{A}^{-1}\cdot\right.$$

$$\mathrm{x}_{n-1}(\mathbb{s}_p)\Big)\left(\mathrm{I}-\Delta\tau_n\mathbb{s}_p\mathbb{A}\right)^{-1}\mathbb{1} \tag{33}$$

Discretization of the heat load in $\mathrm{f}^T(\tau)$ leads to

$$\mathrm{f}^T(\tau_n)=\widehat{\mathbb{V}}^C((\Delta\tau_n\mathbb{A})^{-1})\mathbb{q}_n-\widehat{\mathbb{K}}^C((\Delta\tau_n\mathbb{A})^{-1})T_n+\sum_{p=1}^{N_Q}\mathrm{w}_p\left[\widehat{\mathbb{V}}^C(\mathbb{s}_p)\left(\mathbb{b}^T\mathbb{A}^{-1}\cdot x_{n-1}^{\mathbb{V}^C}(\mathbb{s}_p)\right)-\widehat{\mathbb{K}}^C(\mathbb{s}_p)\left(\mathbb{b}^T\mathbb{A}^{-1}\cdot x_{n-1}^{\mathbb{K}^C}(\mathbb{s}_p)\right)\right]\left(l-\Delta\tau_n\mathbb{s}_p\mathbb{A}\right)^{-1}\mathbb{1} \tag{34}$$

Thus, we get

$$\widehat{\mathbb{M}}_1((\Delta\tau_n\ \mathbb{A})^{-1})[\mathbb{q}]_n=\widehat{\mathbb{M}}_2((\Delta\tau_n\ \mathbb{A})^{-1})[\mathbb{g}_d^T]_n\sum_{p=1}^{N_Q}\omega_\ell\left[\widehat{\mathbb{M}}_2(\mathbb{s}_p)\left(\mathbb{b}^{\mathrm{T}}\mathbb{A}^{-1}\cdot\mathrm{x}_{n-1}^{\mathbb{M}_2}(\mathbb{s}_p)\right)\right.$$
$$\left.\left(-\widehat{\mathbb{M}}_1(\mathbb{s}_p)\left(\mathbb{b}^{\mathrm{T}}\mathbb{A}^{-1}\cdot\mathrm{x}_{n-1}^{\mathbb{M}_1}(\mathbb{s}_p)\right)\right]\left(1-\Delta\tau_n\mathbb{s}_p\mathbb{A}\right)^{-1}\mathbb{1} \tag{35}$$

$$\widehat{\mathbb{M}}_1((\Delta\tau_n\ \mathbb{A})^{-1})[T]_n=\widehat{\mathbb{M}}_2((\Delta\tau_n\ \mathbb{A})^{-1})[\mathbb{g}_n^T]_n\sum_{p=1}^{N_Q}\omega_\ell\left[\widehat{\mathbb{M}}_2(\mathbb{s}_p)\left(\mathbb{b}^{\mathrm{T}}\mathbb{A}^{-1}\cdot\mathrm{x}_{n-1}^{\mathbb{M}_2}(\mathbb{s}_p)\right)\right.$$
$$\left.\left(-\widehat{\mathbb{M}}_1(\mathbb{s}_p)\left(\mathbb{b}^{\mathrm{T}}\mathbb{A}^{-1}\cdot\mathrm{x}_{n-1}^{\mathbb{M}_1}(\mathbb{s}_p)\right)\right]\left(1-\Delta\tau_n\mathbb{s}_p\mathbb{A}\right)^{-1}\mathbb{1} \tag{36}$$

where

$$\widehat{\mathbb{M}}_1=\begin{bmatrix}\widehat{\mathbb{V}}_{DD}^\theta & -\widehat{\mathbb{K}}_{DN}^\theta\\ \widehat{\mathbb{V}}_{ND}^\theta & -(\mathbb{C}_{NN}^\theta+\widehat{\mathbb{K}}_{NN}^\theta)\end{bmatrix}\ \widehat{\mathbb{M}}_2=\begin{bmatrix}\mathbb{C}_{DD}^\theta+\widehat{\mathbb{K}}_{DD}^\theta & -\widehat{\mathbb{V}}_{DN}^\theta\\ \widehat{\mathbb{K}}_{ND}^\theta & -\widehat{\mathbb{V}}_{NN}^\theta\end{bmatrix}$$

4. Numerical results and discussion

BEM was developed using quadratic isoparametric elements, and the 8-point Gauss quadrature algorithm was employed with double precision for the numerical integrations. Alumina was considered in the calculations, with the elastic stiffness coefficients reported in [38].

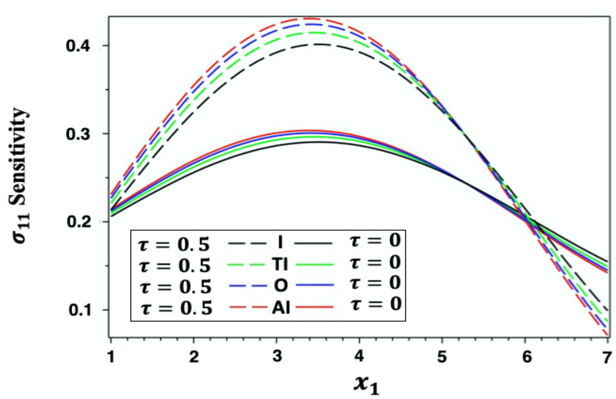

Fig. 1: Thermal stress σ_{11} sensitivity distribution at $\tau=0$ and $\tau=0.5$ for I, TI, O and AI materials.

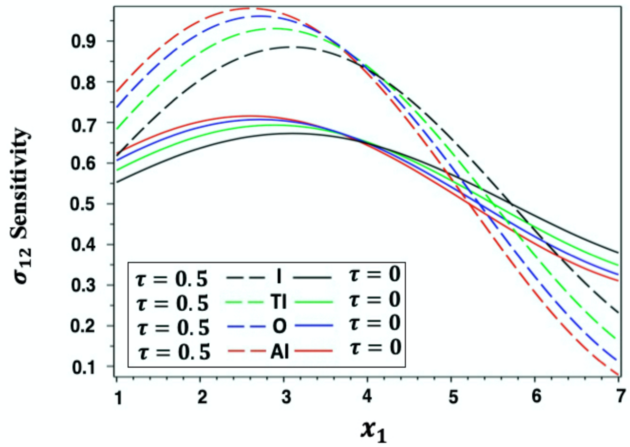

Fig. 2: Thermal stress σ_{12} sensitivity distribution at $\tau=0$ and $\tau=0.5$ for I, TI, O and AI materials.

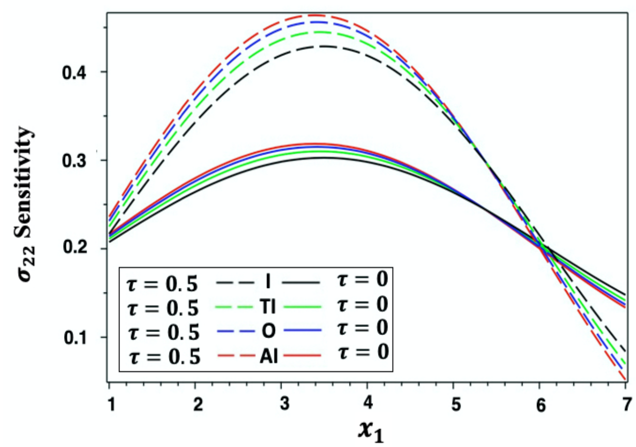

Fig. 3: Thermal stress σ_{22} sensitivity distribution at $\tau=0$ and $\tau=0.5$ for I, TI, O and AI materials.

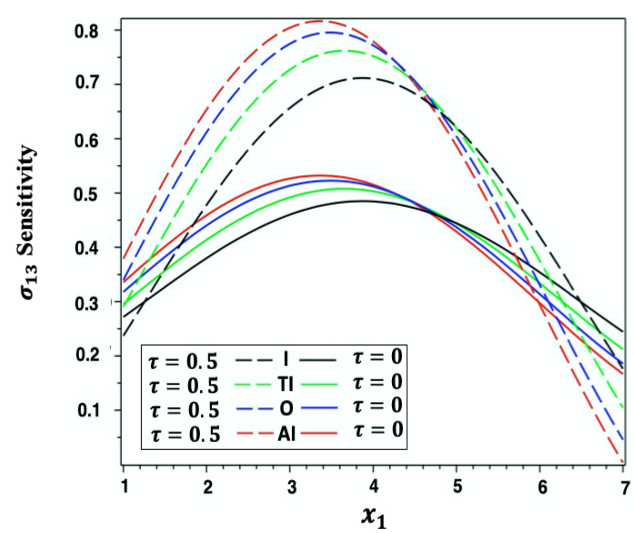

Fig. 4: Thermal stress σ_{13} sensitivity distribution at $\tau=0$ and $\tau=0.5$ for I, TI, O and AI materials.

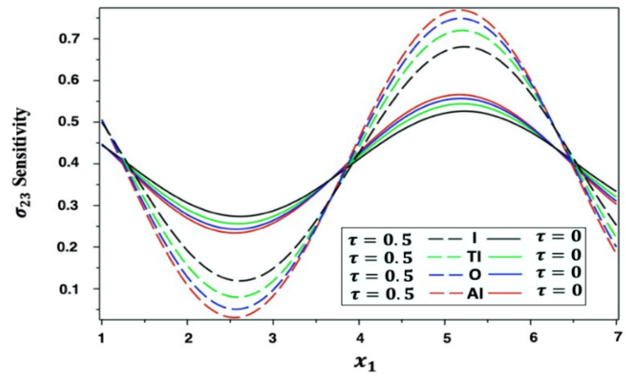

Fig. 5: Thermal stress σ_{23} sensitivity distribution at $\tau = 0$ and $\tau = 0.5$ for I, TI, O and AI materials.

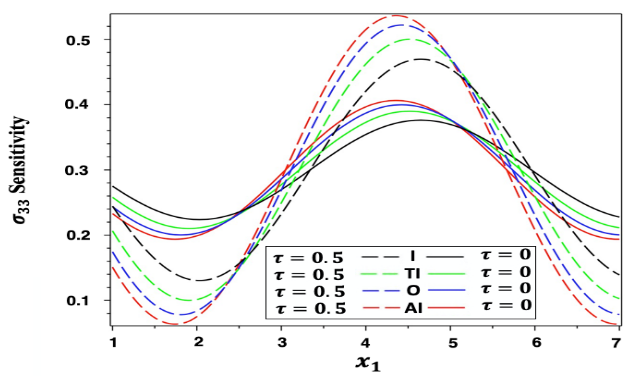

Fig. 6: Thermal stress σ_{33} sensitivity distribution at $\tau = 0$ and $\tau = 0.5$ for I, TI, O and AI materials.

Figures 1-6 depict the distributions of time-dependent $(\tau = 0.5)$ and time-independent $(\tau = 0)$ thermal stresses $\sigma_{11}, \sigma_{12}, \sigma_{22}, \sigma_{13}, \sigma_{23}$ and σ_{33} sensitivity along the x-axis for isotropic (I), transversely isotropic (TI), orthotropic (O), and anisotropic (AI) materials. These figures depict the distinctions between time-dependent and time-independent materials. Furthermore, these figures highlight the differences between the effects of isotropic (I), transversely isotropic (TI), orthotropic (O), and anisotropic (AI) materials.

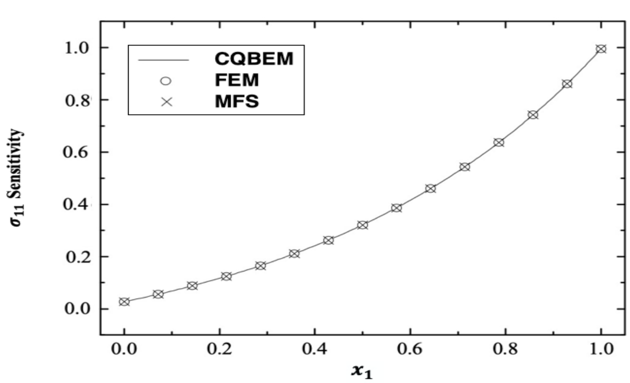

Fig. 7: Thermal stress σ_{11} sensitivity distribution along x_1-axis for CQBEM, FEM, and MFS methods.

Figure 7 compares a special case of the present convolution quadrature boundary element method (CQBEM) thermal stress σ_{11} sensitivity distribution along the x_1-axis to the finite element method (FEM) results of Fang et al. [39] and the method of fundamental solutions (MFS) results of Hematiyan et al. [40]. The current CQBEM, FEM, and MFS all agree quite well. Thus, the proposed method's validity was proven.

5. Conclusions

In this research, we provide a numerical method for computing thermal stress sensitivity that combines convolution quadrature (CQ) and the volume-surface variational formulation of the BEM. The volume integral is approximated in a discretized version of the problem, while the convolution quadrature approach is used to handle the singularity near the boundary. These sensitivity analysis concerns are addressed utilizing the three-dimensional convolution quadrature boundary element method (CQBEM), which allows for non-uniform time increments. The numerical results show that the recommended technique works. The convergence behavior is determined, as expected, by either the time stepping approach or spatial discretization, depending on whether the rate is less. Furthermore, it is shown that the proposed CQBEM approach is superior in certain instances.

References

[1] Chatterjee J., Ma F., Henry D.P., Banerjee P.K. Two- and three-dimensional transient heat conduction and thermoelastic analyses by BEM via efficient time convolution, Computer Methods in Applied Mechanics and Engineering 2007, 196, 2828–2838.

[2] Chaudouet A. Three-dimensional transient thermo-elastic analyses by the BIE method, International Journal for Numerical Methods in Engineering 1987, 24, 25–45, https://doi. org/10.1002/nme.1620240103.

[3] Dargush G.F., Banerjee P.K. Development of a boundary element method for time-dependent planar thermoelasticity, International Journal of Solids and Structures 1989, 25, 999–1021, https://doi.org/10.1016/0020-7683(89)90018-8, ISSN 0020-7683.

[4] Dargush G.F., Banerjee P.K. Boundary element methods in three-dimensional thermoelasticity, International Journal of Solids and Structures 1990, 26, 199–216, https:// doi.org/10.1016/0020-7683(90)90052-W, ISSN 0020-7683.

[5] Dargush G.F., Banerjee P.K. A new boundary element method for three-dimensional coupled problems of consolidation and thermoelasticity, Journal of Applied Mechanics 1991, 58, 28–36, https://doi.org/10.1115/1.2897169, ISSN 0021-8936.

[6] Sládek, V., Sládek, J. Boundary integral equation

method in thermoelasticity part I: General analysis, Applied Mathematical Modelling 1983, 7, 241–253, https://doi.org/10.1016/0307-904X(83)90077-X, ISSN 0307-904X.

[7] Sládek, V., Sládek, J. Boundary integral equation method in thermoelasticity part III: Uncoupled thermoelasticity, Applied Mathematical Modelling 1984, 8, 413–418, https://doi.org/10.1016/0307-904X(84)90047-7, ISSN 0307-904X.

[8] Tanaka, M., Matsumoto, T. and Moradi, M. Application of boundary element method to 3-D problems of coupled thermoelasticity, Engineering Analysis with Boundary Elements 16 (4) (1995) 297–303, https://doi.org/10.1016/0955-7997(95)00074-7, ISSN 0955-7997.

[9] Tanaka, M., Togoh, H. and Kikuta, M. Boundary element method applied to 2-D thermoelastic problems in steady and non-steady states, Engineering Analysis with Boundary Elements 1 (1) (1984) 13–19.

[10] Tosaka, N. and Suh, I.G. Boundary element analysis of dynamic coupled thermoelasticity problems, Computational Mechanics 1991, 8, 331–342, https://doi.org/ 10.1007/BF00369891, ISSN 1432-0924.

[11] Park, K.-H. and Banerjee, P.K. Two- and three-dimensional transient thermoelastic analysis by BEM via particular integrals, Internat. J. Solids Struct. 2002, 39, 2871–2892, https://doi.org/10.1016/S0020-7683(02)00125-7, ISSN 0020-7683.

[12] Fahmy, M. A., M. O .Alsulami, A. E. Abouelregal (2023) Three-Temperature Boundary Element Modeling of Ultrasound Wave Propagation in Anisotropic Viscoelastic Porous Media. Axioms 2023, 12, 473; https://doi.org/10.3390/axioms12050473

[13] Richard B. Hetnarski, M. Reza Eslam, Thermal Stresses – Advanced Theory and Applications, volume 158 of Solid mechanics and its applications, Springer (2009).

[14] Fahmy, M. A. and Toujani, M. Fractional Boundary Element Solution for Nonlinear Nonlocal Thermoelastic Problems of Anisotropic Fibrous Polymer Nanomaterials. Computation 2024, 12, 117. Doi: https://doi.org/10.3390/computation12060117

[15] Fahmy, M. A. BEM Modeling for Stress Sensitivity of Nonlocal Thermo-Elasto-Plastic Damage Problems. Computation 2024, 12, 87. Doi: https://doi.org/10.3390/computation12050087

[16] Fahmy, M. A. and Alzubaidi, M. H. M. A boundary element analysis of quasi-potential inviscid incompressible flow in multiply connected airfoil wing. Journal of Umm Al-Qura University for Engineering and Architecture 2024. Doi: https://doi.org/10.1007/s43995-024-00063-3

[17] Fahmy, M. A. A time-stepping DRBEM for nonlinear fractional sub-diffusion bio-heat ultrasonic wave propagation problems during electromagnetic radiation. Journal of Umm Al-Qura University for Applied Sciences 2024. https://doi.org/10.1007/s43994-024-00178-2

[18] Fahmy, M. A. and Jeli, R. A. A. A New Fractional Boundary Element Model for Anomalous Thermal Stress Effects on Cement-Based Materials. Fractal and Fractional 2024, 8, 753. https://doi.org/10.3390/fractalfract8120753.

[19] Fahmy, M. A. and Almehmadi, M. M. Fractional Dual-Phase-Lag Model for Nonlinear Viscoelastic Soft Tissues. Fractal and Fractional 2023, 7, 66. https://doi.org/10.3390/fractalfract7010066.

[20] Fahmy, M. A. A Nonlinear Fractional BEM Model for Magneto-Thermo-Visco-Elastic Ultrasound Waves in Temperature-Dependent FGA Rotating Granular Plates. Fractal and Fractional 2023, 7, 214. https://doi.org/10.3390/fractalfract7030214.

[21] Fahmy, M. A. and Almehmadi, M. M. Boundary element analysis of rotating functionally graded anisotropic fiber-reinforced magneto-thermoelastic composites, Open Engineering 2022, 12, 313–322. Doi: https://doi.org/10.1515/eng-2022-0036

[22] Fahmy, M. A. Fractional Temperature-Dependent BEM for Laser Ultrasonic Thermoelastic Propagation Problems of Smart Nanomaterials. Fractal and Fractional 2023, 7, 536. https://doi.org/10.3390/fractalfract7070536

[23] Fahmy M. A. A new convolution variational boundary element technique for design sensitivity analysis and topology optimization of anisotropic thermo-poroelastic structures, Arab Journal of Basic and Applied Sciences 2020, 27, 1-12. Doi: https://doi.org/10.1080/25765299.2019.1703493

[24] Lubich, C. Convolution quadrature and discretized operational calculus, I. Numerische Mathematik 1988, 52, 129–145.

[25] Lubich, C. Convolution quadrature and discretized operational calculus, II. Numerische Mathematik 1988, 52, 413–425.

[26] Lopez-Fernandez, M., Sauter, S. Generalized convolution quadrature with variable time stepping, IMA Journal of Numerical Analysis 2013, 33, 1156–1175, https://doi.org/10.1093/imanum/drs034.

[27] Lopez-Fernandez, M., Sauter, S. Generalized convolution quadrature with variable time stepping. part II: Algorithm and numerical results, Applied

Numerical Mathematics 2015, 94, 88–105.

[28] Lopez-Fernandez, M., Sauter, S. Generalized convolution quadrature based on Runge-Kutta methods, Numerische Mathematik 2016, 133, 743–779, https://doi.org/10.1007/s00211-015-0761-2.

[29] Nowacki, W. Dynamic Problems of Thermoelasticity, Nordhoff, Leyden, 1975.

[30] Fahmy, M. A. A time-stepping DRBEM for the transient magneto-thermo-visco-elastic stresses in a rotating non-homogeneous anisotropic solid, Engineering Analysis with Boundary Elements 2012, 36, 335-345. Doi: https://doi.org/10.1016/j.enganabound.2011.09.004

[31] Aliabadi, M.H. The Boundary Element Method: Applications in Solids and Structures, vol. 2, J. Wiley & Sons, 2002.

[32] Manticˇ, V. A new formula for the C-matrix in the somigliana identity, Journal of *Elasticity* 1993, 33, 191–201.

[33] Duffy, M.G. Quadrature over a pyramid or cube of integrands with a singularity at a vertex, SIAM Journal on Numerical Analysis 1982, 19, 1260–1262.

[34] Han, H. The boundary integro-differential equations of three-dimensional Neumann problem in linear elasticity, Numerische Mathematik 1994, 68, 269–281.

[35] Leitner M. and Schanz M. Generalized convolution quadrature based boundary element method for uncoupled thermoelasticity. Mechanical Systems and Signal Processing 2021, 150, 107234. Doi: https://doi.org/10.1016/j.ymssp.2020.107234

[36] Abreu, A.I., Canelas, A., Sensale, B., Mansur, W.J. CQM-based BEM formulation for uncoupled transient quasistatic thermoelasticity analysis, Engineering Analysis with Boundary Elements 2012, 36, 568–578, https://doi.org/10.1016/j.enganabound.2011.10.003, ISSN 0955-7997.

[37] Schanz, M. Wave Propagation in Viscoelastic and Poroelastic Continua: A Boundary Element Approach, in: volume 2 of Lecture Notes in Applied Mechanics, Springer-Verlag, Berlin, Heidelberg, New York, 2001, https://doi.org/10.1007/978-3-540-44575-3.

[38] Huntington, H.B., 1958. The Elastic Constants of Crystals. Academic Press, New York.

[39] Fang, L., Su, F., Kang, Z, Zhu, H. Finite element (FE) analysis of thermal stress in production process of multi-layer lining ladle. Case Studies in Thermal Engineering 2024, 57, 104307. https://doi.org/10.1016/j.csite.2024.104307

[40] Hematiyan, M.R., Mohammadi, M., Tsai C.C. The method of fundamental solutions for anisotropic thermoelastic problems. Applied Mathematical Modelling 2021, 95, 200-218. https://doi.org/10.1016/j.apm.2021.02.001